PACKAGING OF OPTICAL COMPONENTS AND SYSTEMS

In this article, several types of semiconductor optical components are introduced, and packaging of optical components and systems will be discussed. Specifically, three common types of optical sources will be addressed: light emitting diodes (LED), edge-emitting semiconductor lasers, and vertical cavity surface emitting lasers (VCSEL).

Almost all commercial LEDs and laser diodes operate at wavelengths between 400 nm to 1.6 μm. Visible LEDs are commonly used for display purposes. Visible laser diode sources are used for optical data storage, bar code scanners, pointers, and laser printers. Near infrared laser diodes at 780 nm are used for compact disk (CD) players, CD ROMs, and laser printers. In addition, laser diodes at 780 nm and 850 nm are used for short distance optical interconnects for their low volume cost. Laser diodes at 808 nm are specifically designed to pump solid state lasers. Laser diodes at 980 nm are mostly designed to pump Er-doped fiber lasers and amplifiers. The sources for long distance optical communications most often operate at infrared wavelengths near 1320 nm or 1550 nm because standard fibers have minimum dispersion at 1320 nm and minimum loss at 1550 nm. VCSELs with reasonable performances are currently limited to operate at around 650 nm − 980 nm.

As with any semiconductor device, discrete or integrated, an interface must be made with the outside world for signal input and output. The platform for the interface is typically called the package. The package allows electrical and optical connections to the semiconductor in a form that allows handling and protection to the semiconductor. Initial optoelectronic packages were borrowed from the electronics industry in the form of a TO-can (which stands for Transistor Outline) designed in the early 1960s. The TO-can is still a popular package platform today for both laser diodes and photodiodes and has been modified over the years for optoelectronics to become the highest volume laser package to date. Also, in the early 1960s, the plastic transistor package was developed that has since become the mainstay of the LED market. More recent optimizations to the package design in LEDs have utilized the electronics industries Plastic DIP (dual in-line pin) package developed also in the late 1960s that is commonly known as the p-dip. Using similar transfer molded materials, today's LED packages are much smaller than the original transistor designs and are known as plastic surface mount packages or SMTs. As the technology improves, so does the package platform, as evidenced by the trend in high performance laser diodes used in the telecommunications industry. The stringent criteria put on the package in terms of lifetime, hermaticity, the environmental design forced designers in the late 1970s and early 1980s to develop the butterfly package. The butterfly package allows for pig-tailing fibers, mounting of laser diodes, and their associated assessories in a small hermatic container that has a dual in-line pin configuration. This type of package is very popular today with cost insensitive applications such as a single mode fiber for telecommunications. It is the success in terms of performance and commercialization that has driven technologists today to find novel methods to reduce the cost structure of the butterfly platform while retaining some of the excellent features. Having good performance with a low assembly cost structure has been the drive of laser packaging in the 1990s that has lead engineers to focus on a new technology that is based on silicon wafers to mount the optoelectronic devices with the metrics of butterfly performance with the manufacturing ease of TO-cans, p-dips, and simple surface mount platforms.

A detailed discussion of laser and LED sources and the common package platforms could easily fill a book by itself. For introduction purposes, some of the fundamentals of this technology will be presented. The interested readers are referred to some of the many good treatments in the literature (1–4).

OPTICAL COMPONENTS

In this section, device structures of LEDs, edge emitting lasers, and vertical cavity surface emitting lasers (VCSELs) will be introduced. The device packaging related to these optical sources will be addressed later.

Light Emitting Diodes

Light emitting diodes (LED) emit light through carrier injection and electron-hole radiative recombination process. When in forward bias, electrons are excited from the valence band into the conduction band by minority carrier injection across a semiconductor *p–n* junction. When many electrons are accumulated in the conduction band and many holes are accumulated in the valence band, those carriers will recombine and photons are emitted.

The LED material selection is dependent on the desired wavelength of light to be emitted. The use of LEDs can be divided into two broad categories: (1) as a light source for short-distance optical-fiber communications and (2) as a light indicator for display purposes. Because the Rayleigh scattering loss in fibers decreases with wavelength according to λ^{-4}, compound-semiconductor alloys such as $Ga_{1-x}Al_xAs$ and $Ga_{1-x}In_xAs_{1-y}P_y$, which cover the wavelength range 0.80 to 1.55 μm, are most suitable for optical fiber communications. Display indicators, on the other hand, require sources emitting in the visible region. GaP is suitable for this purpose because it has emission peaks in the red and green, two of the three primary colors, in addition to the infrared peak. The red or green peak can be enhanced relative to the others by controlling the impurities. High brightness red and yellow LEDs based on direct bandgap InGaP have also been demonstrated and commercialized. More recently, LEDs based on GaN materials have improved the emission efficiency in the blue dramatically, and the use of InGaN may extend the III-nitride based LED emission wavelength into the red. Now, there is a potential that a monolithic true color display can be built using red, green and blue LEDs on a same substrate.

Figure 1 shows the cross-section of a surface-emitting LED consists of a *p–n* junction, with a controlled concentration profile between the *p*-typed and *n*-typed material. The substrate in this example is GaAs. Other III-V compounds, such as GaP, may be appropriate depending on the desired wavelength of light to be emitted. The substrate layer and the graded layer above are *n*-type doped. A constant layer caps the graded layer and is capped in turn by a dielectric material such as silicon nitride. The *p* region of the *p–n* junction is formed by the diffusion of Zn doping into an opening in the dielectric. The *p–n* junction is contacted on the top by a metal such as gold, AuBe, or aluminum contacting the *p*-type, diffused Zn-doped region. The *n*-type region is contacted on the backside, with a metal such as AuSn or AuGe in contact with the *n*-doped substrate. In some green and yellow LED designs, an original GaAs substrate is replaced with a GaP fused substrate so that the LED can collect more of the lambertian light and direct through the transparent GaP substrate.

Device characteristic curves for LEDs include the forward current-vs.-applied voltage curve, and the light emission or luminous intensity vs. forward current curve. Other useful characteristics in optoelectronic applications include the spectral distribution and the luminous intensity vs. temperature and angle, the latter due to the need to couple into a medium such as optical fiber. An example of each is shown in Fig. 2. The spectral distribution of an LED is always wider than that of a laser.

Device Structure: Lasers

Edge emitting semiconductor lasers have been around for more than 30 years. Semiconductor lasers were first reported in 1962 (5–8). Initial devices were based on forward biased GaAs *p–n* junctions. Optical gain was provided by electron-hole recombination in the depletion region, and optical feedback was provided by polished facets perpendicular to the junction plane. This type of homojunction design meant that the carrier confinement of those lasers was poor, and the high laser threshold prohibited laser operation at room temperature. The concept of using wider bandgap material as one or both cladding layers to improve the laser carrier confinement and thus to reduce the leakage current was first proposed in 1963 (9). Optical mode confinement was also expected to improve because a larger refractive index of the center active layer would provide a waveguide effect. Seven years later, a continuous wave (CW) GaAs/AlGaAs double heterojunction (DH) semiconductor laser operating at room temperature was demonstrated using a liquid phase epitaxial (LPE) growth technique (10,11). Commercial applications of edge emitting semiconductor lasers have since become practical. Today, the worldwide semiconductor laser annual sales revenue has exceeded $400 million (12).

Two types of lasers have been extensively studied. They include GaAs based near infrared $Al_yGa_{1-y}As/Al_xGa_{1-x}As$ (x >

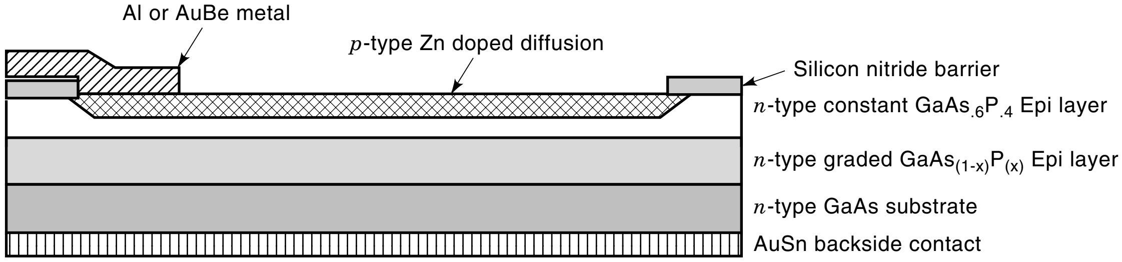

Figure 1. Cross-section of a surface-emitting LED.

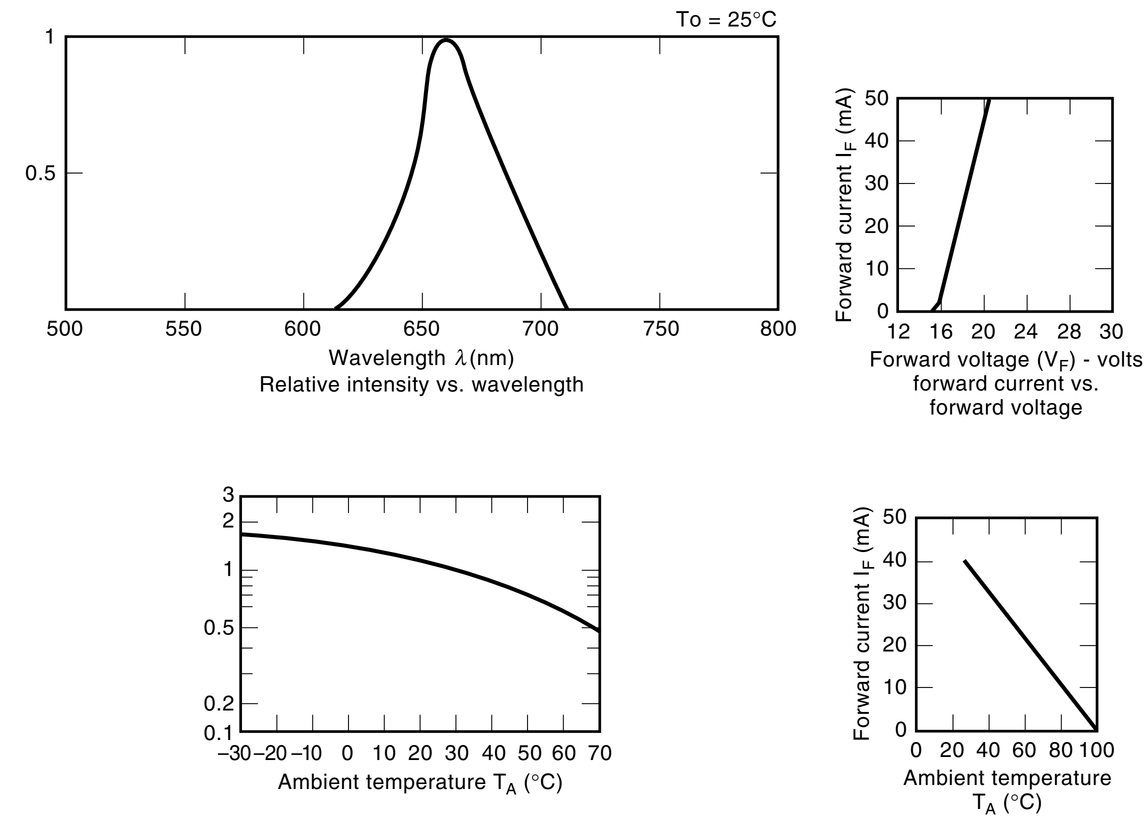

Figure 2. Characteristics of a red visible LED.

y ≥ 0) and InP based long wavelength $In_xGa_{1-x}As_yP_{1-y}$/InP DH edge emitting semiconductor lasers. The epitaxial structures for both types of lasers are similar. They are usually *n–p–p* type, *n–i–p* type, or *n–n–p* type. LPE used to be the dominant epitaxial growth technique during the 1970s and early 1980s for high quality semiconductor laser material growth but has gradually been taken over predominantly by metal organic chemical vapor deposition (MOCVD) techniques. Molecular beam epitaxy (MBE) is also a growth technique that has been used to demonstrate semiconductor lasers in research and development environments with a limited success commercially. A GaAs/$Al_xGa_{1-x}As$ DH laser is shown in Fig. 3, consisting of a multiple of compound semiconductor layers grown on a *n*-type GaAs substrate. The *p*-type active layer of the GaAs

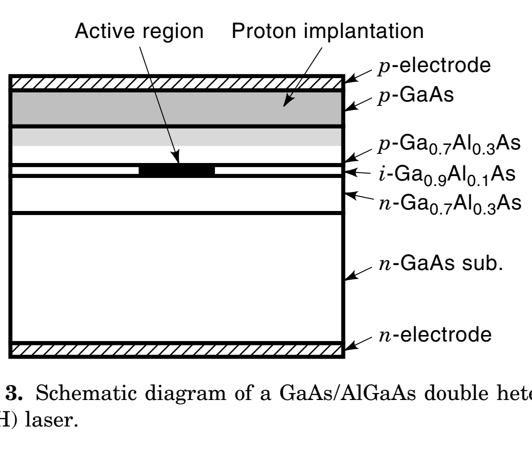

Figure 3. Schematic diagram of a GaAs/AlGaAs double heterojunction (DH) laser.

semiconductor laser, in which stimulated emission is amplified, is made of GaAs doped by Be, C, or Zn at 1×10^{17} cm^{-3}. The active layer thickness ranges from 50 Å to 2000 Å. On top of the active layer is a *p*-type $Al_xGa_{1-x}As$ cladding layer doped to 1×10^{18} cm^{-3} using Be, C, or Zn. Below the active layer is a *n*-type $Al_xGa_{1-x}As$ cladding layer doped to 1×10^{18} cm^{-3} using Si, Sn, or Te. Cladding layer thickness usually ranges from 1500 Å to 1 μm. Within each $Al_xGa_{1-x}As$ layer, x is the value of aluminum (Al) mole fraction. When x is 0.3, for example, the energy bandgap of $Al_xGa_{1-x}As$ is about 1.8 eV, 0.4 eV wider than that of the GaAs active layer. When the *p–n* junction is forward biased, electrons in the *n*-type cladding region are injected into the *p*-type active region. With a *p*-type semiconductor of wide bandgap on the other side of the *p–n* junction, the injected minority carriers are mostly confined within the *p*-type active region. This carrier confinement allows population inversion to occur and optical gain to increase efficiently. In addition, the refractive index of GaAs is higher than that of $Al_xGa_{1-x}As$, and this acts like a waveguide to confine the majority of generated light within the GaAs active layer. The light that is not confined and penetrates into the $Al_xGa_{1-x}As$ cladding layers will not be absorbed by the cladding materials because of the wider bandgap and will, therefore, benefit laser action.

The double heterostructure semiconductor laser represents the single largest constituent of today's total semiconductor laser production because of its application in compact disk (CD) players and CD data storage. The current CD laser market volume is greater than 80 million units per year (12). The high volume of this market has driven the unit cost of a pack-

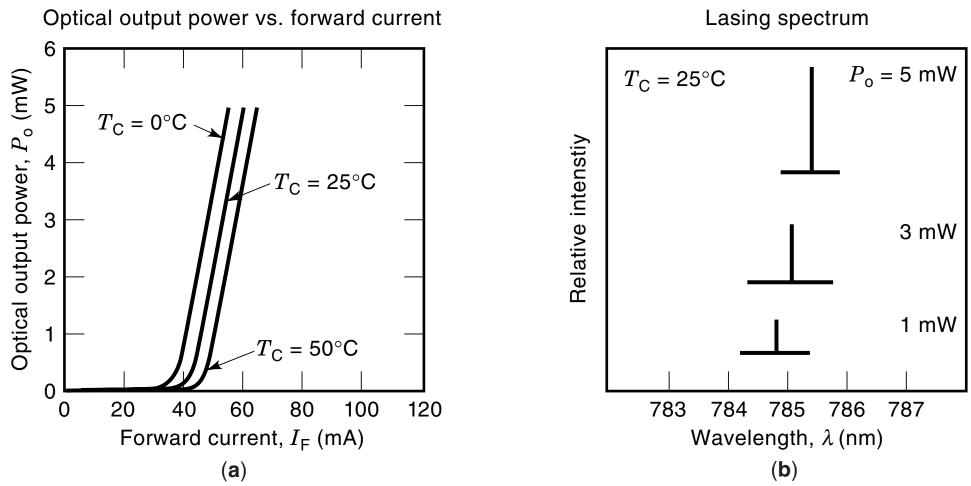

Figure 4. (a) Output power vs. current of a DH laser, and (b) the correspondent laser spectrum.

aged laser to the region of $1, with a large volume pricing in the $1 to $2 range. This has allowed businesses in the fiber optics market to use the low cost CD laser in a historically high cost environment. The CD laser has been used very successfully for short short distance optical data links and has driven laser wavelength specification from 850 nm for using GaAs DH laser down to 780 nm for using CD laser (13,14). Since a CD laser operates at a wavelength of 780 nm, its active layer is made of AlGaAs with an Al mole fraction around 15%. The device fabrication is similar to any other type of DH lasers. Typically, a CD laser has a threshold of 20 mA to 50 mA at room temperature and is operated at an output power of around 3 mW to 5 mW, as shown in Fig. 4. The low threshold CD laser is mostly used for portable consumer electronics powered by batteries. A CD laser is usually designed to operate at multimode or self-pulsation mode in the gigahertz range to reduce the feedback noise from disk light reflection (15). These types of CD lasers, however, will not support multigigabit data communications, as the laser's self-pulsation design is resonant at 1 GHz which adversely affects the noise performance.

When the active thickness of a DH laser is reduced to become comparable to the de Broglie wavelength (16), a quantum mechanical effect starts to occur, and the layer becomes a quantum-well (QW). These QWs have been specifically used to design a new class of single quantum-well (SQW) lasers. Two or more QWs can be placed between the two cladding layers to form a multi-quantum-well (MQW) laser. The layers separating the wells in the MQW laser are called barrier layers. Compared to a SQW laser, the MQW laser has a larger optical mode confinement factor, resulting in lower threshold carrier density and lower threshold current density. In comparison with a DH laser, the QW laser has a smaller active volume, a lower lasing threshold, and a higher differential gain, leading to increased relaxation oscillation frequency and reduced relative intensity noise (RIN). Quantum well lasers with small signal modulation frequencies above 20 GHz have been demonstrated (17,18). High speed semiconductor lasers are important for large bandwidth optical communications, as can be seen by the rapid deployment of optical fibers for transoceanic telecommunication cables and networking backbones throughout the US and the world.

Further reduction of laser threshold current density can be achieved by using a strained QW active layer, such as $In_xGa_{1-x}As$, sandwiched between the GaAs barriers with $0 < x < 0.25$, or between the InP barriers with $x > 0.25$. The biaxial strain caused by the slight lattice mismatch between the two material systems alters the valence band edge by removing the degeneracy of the heavy hole and the light hole, resulting in reduced transparency carrier density and increased modal gain and, thus, reduced threshold current density (19). The strain in the active region also results in a larger differential gain, which helps improve the device operation bandwidth (18,20). Due to critical thickness constraints, the amount of strain in the active region and the active layer thickness, or the number of QWs with strained $In_xGa_{1-x}As$, is limited. To overcome the critical thickness barrier, strain compensated active layers are used to increase the net total active thickness and the differential gain (21–24), thereby improving the optical mode confinement and reducing the laser threshold current density. The strain compensated active structure consists of compressively strained quantum-wells and tensile strained barriers, or vice versa, so that the compressive strain and the tensile strain are mutually compensating for each other. Active layers exceeding the critical thickness can, therefore, be demonstrated without forming any lattice misfit dislocations.

In long haul telecommunicating systems, long wavelength semiconductor lasers are of interest because of the minimum fiber dispersion at 1.3 μm and the minimum fiber loss at 1.55 μm (25). The dispersion shifted fiber will have both the minimum dispersion and the minimum loss at 1.55 μm (26–28). The long wavelength semiconductor lasers are based on $In_xGa_{1-x}As_yP_{1-y}$ active layer lattice matched to InP cladding layers (29,30). By varying the mole fractions x and y, any wavelength ranging between 1.1 μm to 1.6 μm can be selected. An etched-mesa buried-heterostructure (EMBH) laser (31) with a threshold current of around 15 mA at room temperature and a single mode output power of around 10 mW per facet is shown in Fig. 5. One problem with long wavelength semiconductor lasers is the threshold current sensitivity to temperature, at room temperature (small T_0), due to poor carrier confinement and larger Auger nonradiative recombination (32). Improved thermal characteristics (33) and

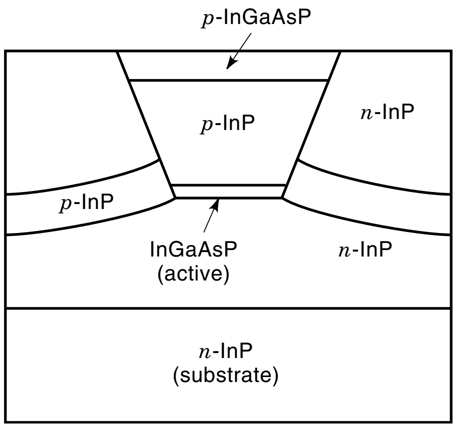

Figure 5. Schematic diagram of a 1.3 μm InGaAsP/InP DH laser epitaxial structure (EMBH).

higher modulation speed (17) have been demonstrated when a MQW active layer is used for the long wavelength semiconductor lasers.

Red visible semiconductor layers operating in the range of 635 nm to 700 nm can find applications in bar-code scanners, laser printers, and laser pointers. They can also be used for plastic fiber data links because of the minimum loss at 650 nm in the plastic fiber (34). With the emerging of digital video disk (DVD) technology for data storage (35), the market demand for both 635 nm and 650 nm semiconductor lasers is expected to soon catch up with the demand for the 780 nm CD lasers. Several material systems, such as AlGaAs (36), InGaAsP (37,38), and InAlGaP (39–41), have been demonstrated to work in this wavelength region, but InAlGaP is regarded as the most appropriate material for it has a large direct energy bandgap while completely lattice matched to a GaAs substrate. High temperature performance and high power operation have been the concerns for InAlGaP visible semiconductor lasers due to carrier leakage into the *p*-cladding layer. Methods utilizing components, such as strained active layer (42,43), off-angle substrate (44,45). MQW active structure (46), and multi-quantum-barrier (MQB) structure (47) have been developed to improve the laser performance.

The new digital video disk (DVD) standard has increased the data storage capacity from 650 Mb to 4.7 Gb on a single sided disk of 12 cm in diameter. This storage capacity increase is attributed more to the tightening of system margin than to the shortening of laser wavelength from 780 nm to 635 nm or 650 nm. A 135 min high definition motion picture, however, needs a storage capacity of 15 Gb. Since the present DVD standard has squeezed the system margin to the minimum, the future generation of DVD technology has to rely to a great extent on laser wavelength shortening to expand the storage capacity in order to maintain the same disk size. Several groups have been investigating green/blue lasers using wide bandgap II–VI compound materials such as ZnCdSe/ZnSSe/ZnMgSSe grown on the GaAs substrate (48–50), and good performance lasers have been demonstrated. The device, however, suffers a serious reliability problem because of stacking fault-like defects that occur at and near the heterointerface between the GaAs substrate and the II–VI materials. Most II–VI semiconductor lasers degrade rapidly within minutes when running at CW. By reducing the grown-in defects, the device CW operation lifetime has been extended to 100 hrs (51), but is not yet long enough for any commercial applications.

Recent advancement in blue light emitting diode (LED) devices based on III-nitride materials (52) has prompted research in the blue/violet semiconductor lasers using InGaN/AlGaN MQW (53,54) or InGaN/GaN DH structures (55). The III-nitride epitaxial structures are grown on c-plane or a-plane sapphire substrates with a thick GaN buffer layer in between because there are no lattice matched substrates available. Lasers on a spinel ($MgAl_2O_4$) substrate have also been demonstrated (56). Crystal quality, p-contact resistivity, carrier and current confinement, and facet mirror reflectivity have been the four major problems in the III-nitride semiconductor laser development (57). Continuous wave operation at room temperature has been achieved at a wavelength around 400 nm by improving the *p*-contact resistance and, thus, reducing the device operating voltage (58). The device has a threshold current of around 3 to 4 kA/cm^2 and a lifetime of about 20 h at 1.5 mW constant power when running at room temperature. The improvement in reliability relies on further reducing the contact resistance and reducing the grown-in crystal defects. The search for a lattice matched substrate will help accelerate the device development cycles. It is expected that lifetimes need to exceed about 10,000 h continuous wave operation at 60°C before serious commercialization is considered.

Vertical-Cavity Surface-Emitting Lasers

Vertical cavity surface emitting lasers (VCSELs) that oscillate perpendicular to the device surface plane were first proposed in the late 1970s (59) to overcome the difficulties facing edge emitting semiconductor lasers that oscillate in parallel to the device surface plane. VCSELs have demonstrated many advantages over edge emitting semiconductor lasers. First, the monolithic fabrication process and wafer scale probe testing as per the silicon semiconductor industry substantially reduces the manufacturing cost because only known good devices are kept for further packaging (60,61). Second, a densely packed two-dimensional (2-D) laser array can be fabricated because the device occupies no larger area than a commonly used electronic device (62). This is very important for applications in optoelectronic integrated circuits (OEIC). Third, the microcavity length allows inherently single longitudinal cavity mode operation due to its large mode spacing. Temperature-insensitive devices can, therefore, be fabricated with an offset between the wavelength of the cavity mode and the active gain peak (63,64). Finally, the device can be designed with a low numerical aperture (NA) and a circular output beam to match the optical mode of an optical fiber, thereby permitting efficient coupling without additional optics (61,65).

A conventional edge emitting semiconductor laser utilizes its cleaved facets as laser cavity reflectors because the length of the active layer is usually several hundred micrometers. The long active length provides sufficient optical gain to overcome the cavity reflector loss even though the reflectivity of the facets is only ~30%. In comparison, a VCSEL needs both of its cavity mirrors to be highly reflective since its active layer is less than 1 μm thick. The first VCSEL was demonstrated with GaInAsP/InP in 1979, which operated pulsed at

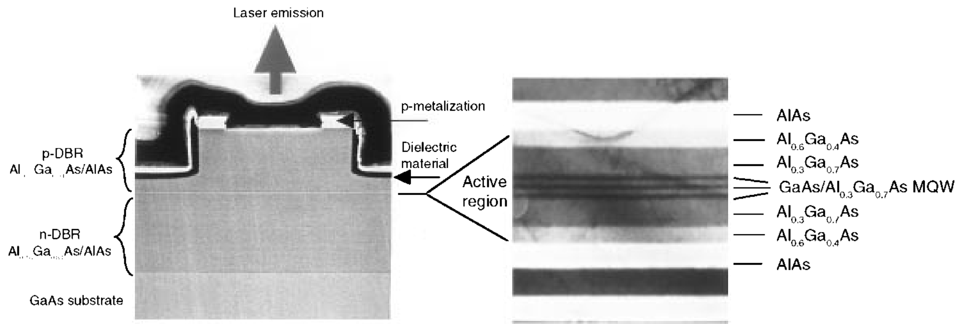

Figure 6. Cross section TEM photo of an etched mesa GaAs VCSEL structure.

77 K with annealed Au at both sides as reflectors (59). A room temperature pulsed operating VCSEL was demonstrated with a GaAs active region in 1984 (66). Room temperature CW operating GaAs VCSELs succeeded by improving both the mirror reflectivity and current confinement (67).

VCSELs are now capable of generating an output power of more than 100 mW with good thermal sinking (68,69). VCSELs with lasing threshold of sub-100 μA (70,71) or wall-plug efficiency of over 50% have been reported using lateral oxidized-Al confinement blocks (72,73). Room temperature CW InGaAsP/InP VCSELs have met some difficulties primary due to a low index difference between GaInAsP and InP, which causes difficulty in preparing a highly reflective monolithic DBR (74). Nevertheless, CW InGaAsP VCSELs at 1.5 μm have been recently reported using GaAs/AlAs DBR mirrors (75,76).

Two dimensional arrayed VCSELs (62,77,78) can find important applications in stacked planar optics, such as the simultaneous alignment of a tremendous number of optical components used in parallel multiplexing lightwave systems and parallel optical logic systems, free space optical interconnects, etc. High power lasers can also be made with phase-locked, 2-D arrayed VCSELs (79,80), but have yet to be commercialized.

The VCSELs being developed today are mostly in the near infrared wavelength range based either on GaAs/AlGaAs or strained InGaAs active materials. GaAs VCSELs at 850 nm are preferred as the light sources for short distance optical communications because either Si or GaAs pin detectors can be used in the receiver end to reduce the total system cost. A typical etched mesa type GaAs VCSEL structure is shown in Fig. 6. It includes three major portions: bottom DBR (diffractive Bragg reflector), active region, and top DBR.

Generally, the epitaxial material is grown by either MOCVD or MBE techniques. The bottom DBR is n-type doped, grown on an n-type doped GaAs substrate. Silicon (Si) and selenium (Se) are two commonly used n-typed dopants. The n-DBR is comprised of 30.5 pair (81,82) of $Al_{0.16}Ga_{0.84}As/AlAs$, which starts and stops with the AlAs layer alternated by the $Al_{0.16}Ga_{0.84}As$ layer. Each DBR layer has an optical thickness equivalent to a quarter of the desired lasing wavelength. The intrinsic cavity region is comprised of two $Al_{0.6}Ga_{0.4}As$ spacer layers and three to four GaAs quantum-wells with each quantum-well sandwiched between two $Al_{0.3}Ga_{0.7}As$ barriers. With the quantum-well width of 100 Å and the quantum barrier width of 70 Å, the lasing wavelength is around 850 nm. The $Al_{0.6}Ga_{0.4}As$ spacer can be replaced by an $Al_xGa_{1-x}As$ spacer with x graded from 0.6 to 0.3 to form a graded index separate confinement heterostructure (GRINSCH). The total thickness of the spacers is such that the laser cavity length between the bottom and the top DBRs is exactly one wavelength or its multiple integer. The p-type doped DBR is grown on top of the active region. It consists of 22 pairs of $Al_{0.16}Ga_{0.84}As/AlAs$ alternating layers which start with an AlAs layer and stops with $Al_{0.16}Ga_{0.84}As$. Like the n-DBR, each layer has an optical thickness of a quarter wavelength. The most common p-type dopants utilized are carbon (C), zinc (Zn) and Beryllium (Be). Typically, C is used for the p-doping in the top DBR when using MOCVD growth techniques with the top several layers doped by Zn for better metalization contact (83). Finally, a GaAs cap is used to prevent the top AlGaAs layer of the p-DBR from oxidation. The cap is high p-doped with Zn as the dopant and is kept to 100 Å thick, as the material will be highly absorptive to the optical mode if it is too thick.

The exact number of quarter wavelength DBR mirror pairs varies from one manufacturer to the other. The function of DBRs in a VCSEL is equivalent to cleaved facets in an edge emitting laser: to reflect part of the laser emission back into the laser cavity and to transmit part of the laser emission as the output. They are, in essence, similar to dielectric mirrors. The n-DBR reflectivity is typically higher than 99.9% at the designed wavelength with a certain bandwidth and the p-DBR reflectivity is typically around 99.5% as the laser output mirror. A typical GaAs VCSEL output power versus input current is shown in Fig. 7 for a mesa diameter of 10 μm and a laser emission aperture of 7 μm.

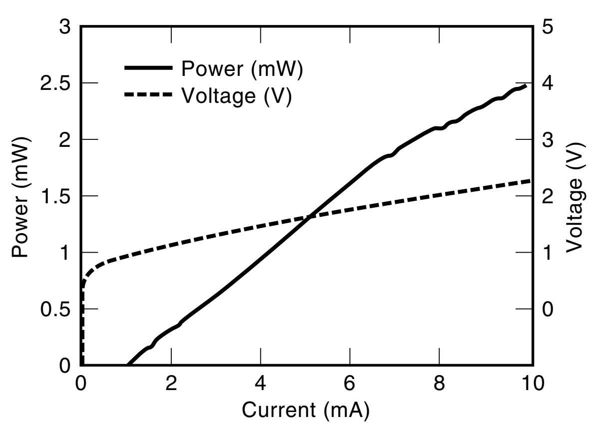

Figure 7. ILV characteristics of a mesa type GaAs VCSEL with the mesa diameter of 10 μm and the emission aperture of 7 μm. The laser wavelength is around 850 nm.

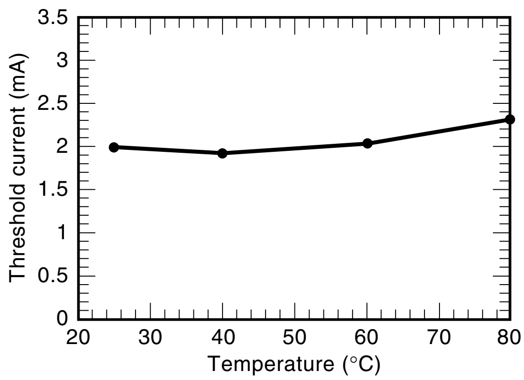

Figure 8. Threshold current of a typical GaAs VCSEL varying with ambient temperature with minimum threshold current at 40°C.

Within the microcavity structure of a VCSEL, only one Fabry Perot cavity mode exists in the designed DBR reflective bandwidth. A laser can only be sustained at the wavelength of the cavity mode. Clearly, a temperature insensitive VCSEL can be demonstrated by taking advantage of the microcavity mode characteristic (63). Typically, the peak of the active gain profile shifts with the temperature at a rate of 3 to 5 Å/°C, and the cavity resonant mode shifts at a rate of 0.5 to 1 Å/°C (84). If the resonant cavity mode is designed to initially sit at the longer wavelength side of the gain profile, the gain peak will gradually walk into the cavity mode with the rise of temperature. Conversely, the gain peak usually decreases in wavelength with the temperature. Together, the actual gain for the VCSEL cavity mode will vary little with temperature, and the VCSEL threshold current will stay almost constant within a certain temperature range. This temperature insensitivity allows the VCSEL to be designed to operate optimally at the system temperature mid-point region. For example, with modest speed optical data links, the VCSELs can be designed to operate with minimum threshold current at around 40°C in a required working range of 0° to 70°C, as shown in Fig. 8 (64,85). The system can be implemented without any auto power control (APC) circuitry, thereby simplifying the packaging and reducing the system cost (61). The application of this method has also allowed the demonstration of VCSELs operating at a record high temperature of 200°C (82).

VCSELs of superior performances have been demonstrated using strained InGaAs operating at around 980 nm as the gain medium (64,86). The strain in the active region provides higher gain that allows lower lasing threshold and higher differential gain that allows larger intrinsic modulation bandwidth. In addition, the InGaAs VCSEL has a wavelength transparent to the GaAs substrate, allowing the light emission toward the substrate side and, thus, allowing epitaxy side down packaging similar to active down packaging in edge emitting lasers. The epitaxy down packaging will more efficiently dissipate heat generated in the *p*-DBR mirror and the active junction region, resulting in lower junction temperature and higher output power. However, 980 nm VCSELs are not preferable for short distance optical data communications because the low cost Si or GaAs PIN detectors cannot be used for the receivers.

Apart from 850 nm VCSELs based on GaAs multi-quantum-wells (MQWs) and 980 nm VCSELs based on strained InGaAs MQWs, VCSELs operating at other wavelengths, such as 780 nm based on AlGaAs MQWs, 650–690 nm based on InAlGaP MQWs, and 1.3 nm to 1.5 nm VCSELs based InGaAsP MQWs have received attention in the research community.

The vast majority of the semiconductor laser market is at 780 nm, which is predominantly used for CD data storage and laser printing. As a result, the development of VCSELs at 780 nm is of strategic importance from a commercial stand point. A typical VCSEL at 780 nm has an epitaxial layer structure similar to that of a VCSEL at 850 nm (87–89). The larger bandgap requirement for 780 nm drives the MQW active region to the AlGaAs ternary system. The active region usually consists of 3 or 4 periods of $Al_{0.12}Ga_{0.88}As$ quantum-wells sandwiched between the $Al_{0.3}Ga_{0.7}As$ barriers. The DBR mirror stack consists of $Al_{0.25}Ga_{0.75}As/AlAs$ with the bandwidth centered at 780 nm. The laser performance of a 780 nm VCSEL is similar to that of a 850 nm GaAs VCSEL. The increased aluminum concentration in both the active region and the DBR mirror stack over that used in the 850 nm VCSEL raises a concern with the 780 nm VCSEL device reliability because of the poor edge emitting semiconductor laser performance at 780 nm. There has been no reliability data published so far for the 780 nm VCSELs, and study is on-going to address the issue.

Red visible VCSELs are of interest because of their potential applications in plastic fiber based optical interconnects, bar-code scanners, pointers, laser printers, and most recently, the DVD format optical data storage. The epitaxy structure of a red visible VCSEL is grown on a GaAs substrate misoriented 6° off (100) plane toward the nearest $|111>$ A or on a (311) GaAs substrate (90–93). It consists of 3 to 4 periods of $In_{0.56}Ga_{0.44}P$ QWs with InAlGaP or InAlP as barriers, InAlP as both *p*-type and *n*-type cladding layers, and two DBR mirrors. The active QW layer is either tensile or compressive strained to enhance the optical gain. Typically, the QW thickness is 60 Å to 80 Å, and the barrier thickness is 60 Å to 100 Å. The total optical cavity length including the active region and the cladding layers ranges from one wavelength or its multiple integer up to eight wavelengths. The DBR mirrors are composed of either InAlGaP/InAlP or $Al_{0.5}Ga_{0.5}As/AlAs$. The $Al_{0.5}Ga_{0.5}As/AlAs$ DBR mirror performs better because of a relatively larger index difference between the two DBR constituents, thus, a higher reflectivity and a wider bandwidth. In general, because the index difference between $Al_{0.5}Ga_{0.5}As$ and AlAs is much smaller than that used for the 850 nm VCSELs, more mirror pairs are needed to achieve the required DBR reflectivity. Generally, more pairs in the DBR mirror introduce higher series resistance, and thus, more heat will be generated in the active region. The active junction temperature will, therefore, be higher. Currently, submilliampere threshold red VCSELs have been demonstrated. More than 5 mW output power from a red VCSEL has also been reported. Unfortunately, the carrier confinement of the red visible VCSELs is poor because of the smaller bandgap offset between the quantum-well and the barrier and between the active and the cladding. Therefore, the red visible VCSELs are extremely temperature sensitive, and more studies are needed to improve the red visible VCSEL high temperature performances. VCSELs with wavelengths shorter than 650 nm pose more problems because of even worse carrier confinements. Designing a red visible VCSEL that can effectively

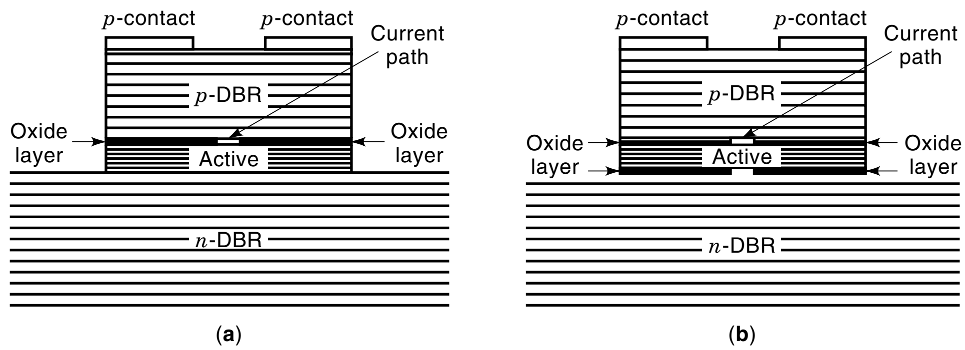

Figure 9. VCSEL with native aluminum oxide for lateral current confinement. (a) Current confinement on p-side, and (b) current confinement on both p-side and n-side.

confine the carriers in the active region is a challenging research topic.

Long wavelength VCSELs at 1.3 μm and 1.55 μm have drawn attention because of their potential applications in telecommunications and medium to long distance data links, such as local area networks (LAN) and wide area networks (WAN), where single mode characteristics are required. The long wavelength VCSELs are based on InP substrates, with InGaAsP MQWs used as active media. However, the lattice matched monolithic InGaAsP/InP DBR mirrors do not have sufficient reflectivity for the long wavelength VCSELs because of the small index difference between the two DBR mirror pair constituents, InGaAsP and InP. In addition, the Auger recombination induced loss becomes evident due to smaller energy bandgap for the long wavelength VCSELs. To overcome the difficulty, dielectric mirrors with 8.5 pairs of MgO/Si multilayers and Au/Ni/Au on the p-side and six pairs of SiO_2/Si on the n-side have been used instead of the semiconductor DBR. A continuous wave 1.3 μm VCSEL has, therefore, been demonstrated at 14°C (94). To further improve the device performance, wafer fusing techniques have been adopted to bond GaAs/AlAs DBR mirrors onto a structure with an InGaAsP MQW active layer sandwiched between the InP cladding layers that are epitaxially grown on the InP substrate (95,96). The InP substrate is removed to allow the GaAs/AlAs DBRs to be bonded onto one or both sides of the InGaAsP active region. As the DBR mirrors are either n-type or p-type doped, the completed fused wafer can be processed like a regular GaAs VCSEL wafer. In this way, a 1.5 μm VCSEL has been successfully fabricated that operates CW up to 64°C (75,76). Manufacturing yield and reliability is to be investigated with the VCSEL wafer fusion technique. For commercial interest, the CW operation must at least be driven to the 100°C range for the junction in addition to addition to a number of other issues, such as wall plug efficiency, reliability, and consistency, to name a few. Typically, reliabilities of 100,000 h and above are needed for commercialization of the technology in fiber optic communication applications.

Automatic power control (APC) is one of the important features that is easily accomplished with edge emitting lasers because of the backward emission that can be monitored from the cleaved facet. With VCSELs of wavelength shorter than 870 nm, the laser beam only emits toward the top epitaxy side. The backward emission is absorbed by the GaAs substrate unless the substrate is removed. However, due to the unique vertical stacking feature of VCSELs, a detector can be integrated underneath or above the VCSEL structure during the epitaxy growth (89,97–100). VCSEL operation with APC can be accomplished by monitoring the current variation generated in this detector.

Super low threshold microcavity type VCSELs have been proposed that utilize the spontaneous emission enhancement due to more spontaneous emission being coupled into the lasing mode (101,102). Although a laser without a threshold is theoretically possible when the spontaneous emission coupling efficiency β is made approaching unity, the proposed structures are difficult to make in practice. One of the successful examples in research today is to use oxidized lateral carrier confinement blocks by oxidizing an AlAs layer in the DBR or the cladding regions (70,71,103), as shown in Fig. 9. Typically, sub-100 μA threshold can be achieved with this technique. VCSELs with oxidized mirrors have been demonstrated with extremely simple epitaxy layers (104,105).

High speed data transmission requires that a VCSEL be modulated at multigigahertz. The cavity volume of a VCSEL is significantly smaller than that of an edge emitting laser, resulting in a higher photon density in the VCSEL cavity. The resonance frequency of a semiconductor laser typically scales as the square root of the photon density, thus indicating that a VCSEL has a potential advantage in high speed operation. However, the parasitic series resistance caused by the semiconductor DBR and the subsequent device heating limit the maximum achievable VCSEL modulation bandwidth. Currently, a modulation speed of larger than 16 GHz has been reported with an oxide confined VCSEL at a current of 4.5 mA (106). Modeling results indicate that a gain com-

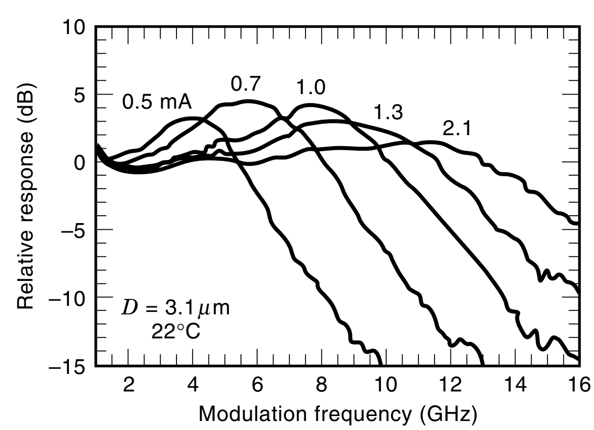

Figure 10. Small signal modulation response of a 3 μm VCSEL at various bias current. The maximum 3-dB bandwidth is about 15 GHz. (After (107)

Figure 11. Several types of plastic molded LED packages.

pression limited oxide VCSEL with a diameter of 3 μm has an intrinsic 3-dB bandwidth of 45 GHz (107) and a measured 3-dB bandwidth of 15 GHz at 2.1 mA due to the parasitic resistance and the device heating, as shown in Fig. 10.

PACKAGING

LED Packaging

Hundreds of millions of LEDs are sold annually in the world, 90% of which are packaged using plastic molding technology. A variety of types of LED packaging formats, such as the top emission type, side emission type, and surface mount type are designed to ease the final assembly. Visible discrete LEDs are often used as equipment function indicators. As a result, either clear plastics or color plastics are used as the packaging materials, depending on the final application. IR LEDs are mostly used for optical interconnect, remote control, and sensing. Figure 11 shows several general types of packaged discrete LEDs. The packaging usually starts with mounting LED dies onto aluminum preforms with silver based epoxy. After the wirebond, the chip sets are overmolded with plastics. Finally, the electrical contact pins are separated. As with any high volume manufacturing, the packaging flow is handled automatically in most assembly lines using similar cost effective tooling that is found in the electronics industry.

In addition to being the light indicators, the visible discrete LEDs can find large volume applications in other fields. Compared with incandescent lamps, LEDs are more energy efficient and more reliable, and therefore, LED lamps are ideal light sources for traffic lights and automobile tail lights. The visible discrete LEDs are also becoming more popular for small displays. They are usually packaged in a dot matrix format, as shown in Fig. 12. Full color outdoor displays are another application that consumes large quantities of discrete visible LEDs. For example, a typical VGA grade outdoor display will need at least 1 million discrete LEDs in red, green, and blue colors.

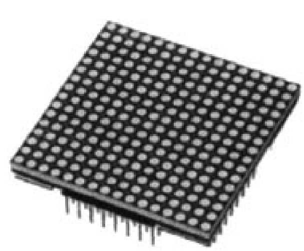

Figure 12. A dot matrix LED package.

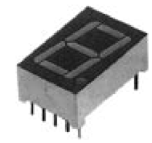

Figure 13. A seven-segment LED package.

The second most important LED application is the seven-segment LED display, which is used to display numerical number and alphabet, as shown in Fig. 13. Seven or more visible LED dies, depending on the brightness requirement and number of digits, are mounted onto a metal preform and wire bonded before going through the plastic molding process.

The development of LED based virtual display has accelerated the development of packaging technology for large LED arrays. Figure 14 shows how a 34K LED array is flip-chip bonded to a thin film fan out conductor pattern on a glass substrate (108). Similar to liquid crystal display (LCD) packaging, either passive or active matrix addressing technology can be adopted in reducing the LED array packaging complexity.

Edge Emitter

In general, edge emitting laser packaging should achieve good thermal conduction, stable optical interface between the laser and fiber/lens if used for optical communications, autopower control capability, and a stable environment such as hermaticity. For applications in optical communications, the packaging cost can be significant because of the need for a thermal electric cooling device, optical isolator, optical modulator, high speed electrical connections, external cavity line width controlling units, and so on. The necessity of using active alignment to couple a laser into a single mode fiber also contributes very significantly to the total packaging cost. Extensive

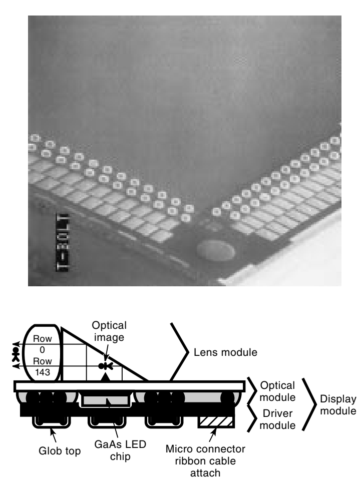

Figure 14. A 34k-LED array flip chip mounted on a transparent glass submount.

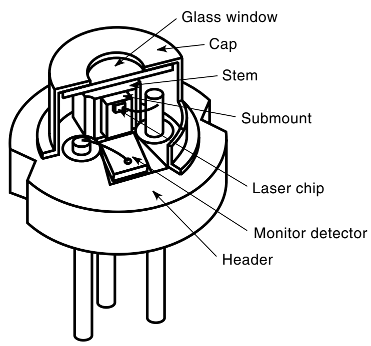

Figure 15. A TO-56 can.

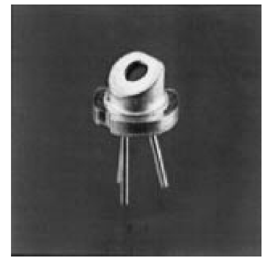

Figure 16. A slanted TO-56 can to reduce the laser noise due to reflected light from the glass window.

studies have been conducted to achieve efficient passive alignment between the laser and the fiber.

There are several basic edge emitting laser packaging technologies with two main commercial categories—TO-can and Butterfly packages. Most commercial semiconductor lasers are packaged using the TO-can technology that was borrowed from the electronics industry. The low cost manufacturability of TO-can allows it to be widely used for many consumer applications such as CD data storage, bar code scanners, laser pointers, laser printers, and serial fiber optic data links. Butterfly (dual-in-line pin) type packages were developed during the 1980s and have since been used predominantly for fiber pig-tailing in the 14 and 20 lead configurations. The butterfly package costs more to manufacture and has mostly been used for long wavelength semiconductor lasers in telecommunication applications as it provides a platform for high reliability design. Plastic molding usually drives down the cost of optoelectronic device packaging dramatically, as is seen from the majority of LED packages, but its application is limited to low power laser diodes because of its disadvantage in heat dissipation and hermaticity. Silicon wafer board type packaging technology has been developed for passive alignment of laser diode to fibers and integrated optoelectronics. The commercialization of silicon wafers board technology is beginning (109). Recently a 14 pin DIL package has been agreed upon by a number of laser suppliers as a standard for optical communication-type edge emitting lasers.

TO-Can. Semiconductor lasers packaged in metal TO-cans dominate today's commercial semiconductor laser market. Earlier, TO-cans had a diameter of 9 mm, but the trend has been turned to use a smaller type TO-56 package with a diameter of 5.6 mm, as shown in Fig. 15. Low thermal impedance TO-3 cans have been used for high power laser diode packaging for their high thermal capacity. Both the TO-56 can headers and TO-56 can lids are manufactured using standard low cost metal stamping process. The laser chip is usually mounted upside down on a Si submount with AuSn or other types of high temperature solder. Electrical transmission lines are deposited on the submount for electrical contacts. The Si submount on which the laser chip has been attached is then mounted vertical with In-solder onto a copper heat sink that sits on the header. In some designs, the laser ship is directly mounted upside down onto the copper heat sink without any Si submount. The TO-header is based on copper, iron, or nickel, depending on the heat dissipation and cost requirements. Both the heat sink and the header can be plated with gold for better heat dissipation.

If autopower control (APC) is needed, a silicon PIN detector is directly mounted onto the header with a Sn- or In-solder to receive the laser emission from the back facet. The detector on the header is tilted to avoid any reflected light from coupling directly back into the laser, thus destabilizing the laser operation. The detector can sometimes be made directly on the silicon submount that will detect one-half of the cone shaped backward laser emission for the last power monitoring.

Gold wire bonding process is traditionally used to connect electrodes of semiconductor lasers and photodiodes to the corresponding posts of the TO-headers. Depending upon applications, the semiconductor laser cathode can be either in common with the monitoring photodiode cathode or in common with the monitoring photodiode anode. Finally, a lid is hermetically sealed onto the header using welding. Hermetic sealing is needed to improve the laser reliability. The laser emits through a glass window of the lid which is typically sealed and attached by a glass frit. The glass window is AR coated to reduce the backward reflection that is detrimental to the laser signal-to-noise ratio (SNR). A slanted lid can be used to steer the backward reflection light away from entering the laser cavity, as shown in Fig. 16.

Butterfly Package. Dual-in-line butterfly laser packages (Fig. 17) are generally used for optical communications. Laser

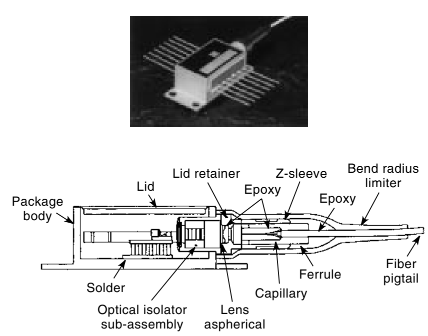

Figure 17. A dual-in-line butterfly package for long wavelength semiconductor lasers.

is coupled into a single mode fiber with a core diameter of less than 10 μm. Butt-coupling (or direct coupling) is one of the commonly used active alignment techniques for fiber pigtailing. In this scheme, a laser chip is first mounted onto a subcarrier and turned on. An optical fiber is brought close to the emission end of the laser to achieve the best coupling efficiency and then secured onto the subcarrier. The butt-coupling usually has a loss of more than 3 dB because of the poor matching in numerical aperture (NA) between the laser beam and the fiber. The coupling efficiency can be improved dramatically by inserting a lens between the laser and the fiber (110). Many types of lenses can be used, but a gradient-index (GRIN) lens is among the best in performances (111). An integrated ball lens can be made directly using the glass fiber tip, and relatively good coupling has been achieved (112). Because edge emitting semiconductor lasers are very sensitive to ambient temperature, a high end telecommunication laser or laser subassembly is always mounted on a thermal-electric (TE) cooler to maintain constant operation temperature. A butterfly package, therefore, includes contact pins symmetrically distributed along the two long axial sides that allow dc prebias and RF modulation to the laser diode, dc bias to the laser power monitoring photodiode, dc bias to the TE cooler, contact to the thermistor, and both RF and case grounding. Some pins of the standard butterfly package (14 & 20 pins) are not used. An uncoated fiber facet tends to reflect some portion of the incoming laser signal back into the laser cavity, increasing the laser noise and reducing the side mode suppression ratio. Optical isolators have been used in most of the high end telecommunication laser packages to block the reflected laser beam. On lower cost packages either the fiber or the laser facet is slightly angled to suppress back reflections. Generally, a butterfly package can be designed to accommodate the multi-Gigabit bandwidth requirement with a wide variety of technical performance specifications.

CD lasers at 780 nm are commercially available at a substantially low price. A standard TO-can packaged CD laser can be coupled through a ball lens or a GRIN lens into a multimode fiber as an alternative approach to a butterfly laser package to provide a low cost, short distance data communication solution at several hundred megahertz or up to 1 GHz (13,14). Usually, a lens is mounted in a cylindrical receptacle (commonly known as an optical subassembly), with room to fit a TO-can packaged laser, as shown in Fig. 18. The multimode optical fiber is connected to the other end of the receptacle.

Silicon Wafer Board. Silicon wafer board packaging technology has been driven by the need to package arrays of lasers to arrays of fibers. Individually aligning fibers to arrays of

Figure 18. Serial link package.

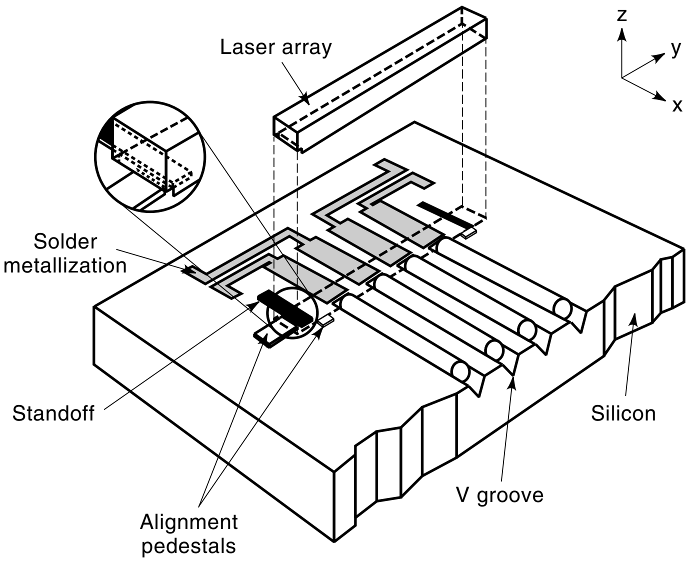

Figure 19. A four-channel laser array mounted on a V-grooved Si waferboard using the passive alignment concept.

edge emitting lasers is a major assembly effort and typically, has been almost hand assembled using active alignment. The need to align an edge emitting semiconductor laser array to pigtailed fibers without any active alignment is critical in the drive to reduce packaging costs. Passive coupling alignment is preferred to increase the packaging throughput and to reduce the manufacturing cost. A 4-channel silicon wafer board package is shown in Fig. 19 (113). Four V-grooves have first been fabricated uniformly spaced apart on the Si waferboard. The V-groove spacing is determined by the laser spacing of a 4-channel laser array. The laser array is flip chip mounted adjacent to the end of the V-grooves with its position aligned to the marks on the Si waferboard. A self-alignment technique can also be used to position the laser chip using solder reflow, as shown in Fig. 20 (114). Four fiber cores are then placed into the V-grooves on the Si waferboard with their input ends leaning against the end of the V-grooves. A Si cover-carrier with V-grooves for the fiber cores and a space for the laser chip is placed back onto the Si waferboard using optical glue to secure the whole package. No lenses are used between the lasers and the fibers as the laser emission facets are right against the fiber input ends, and their relative positions are predetermined with very high placement accuracy.

VCSEL Packaging

Current commercial VCSELs are predominantly developed for optical interconnect applications. The VCSEL packaging is, therefore, centered around how to effectively interface between VCSELs with optical fibers at a substantially low cost. Fortunately, the VCSEL has a circular beam shape; it can be efficiently coupled into an optical fiber. A single VCSEL can be packaged in the same way as a surface emitting light emitting diode (LED) on either a TO-type can or a plastic molded leadframe (Fig. 21). A plastic molded lens can be integrated to the leadframe surface mount type package to adjust the laser beam divergence angle, thus to match the NA of the fiber for better coupling efficiency.

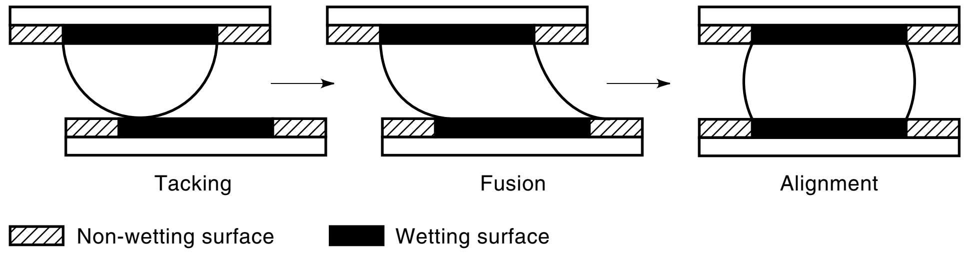

Figure 20. Self alignment using solder reflow.

One-dimensional (1-D) or two-dimensional (2-D) array capabilities are a unique advantage of VCSEL technology. The OPTOBUS™ data link package is an example how a 1-D VCSEL array can be packaged to couple into multimode fibers (61), as shown in Fig. 22. The OPTOBUS™ data link package uses a 1 × 10 VCSEL array. A leadframe with 10 copper leads for the VCSEL anodes and two copper leads for the VCSEL cathodes is first embedded into a 10-channel polymer waveguide GUIDECAST™ optical interface unit (OIU). The 12 leads are bent toward the input end of the GUIDECAST™ OIU for direct chip attachment of a VCSEL array onto the leads. The VCSEL anodes and cathodes are all fabricated on the VCSEL emission side. The VCSEL electrical contacts are plated with Au. A robot is used to flip-chip mount and passively align the VCSEL array onto the GUIDECAST™ OIU with a placement accuracy of several micrometers, enough to guarantee an accurate alignment of a VCSEL of an emission aperture of 5–15 μm in diameter onto a GUIDECAST™ OIU waveguide channel of dimensions on the order of 40 μm × 40 μm. The electrical contact between the VCSELs and the GUIDECAST™ OIU copper leads are achieved using conductive epoxy. The gap between the VCSELs and the waveguide may be underfilled with materials of the same composition as the GUIDECAST™ OIU to secure a robust attachment of the VCSEL array onto the GUIDECAST™ OIU. The GUIDECAST™ OIU copper leads also function as thermal heat sinks to dissipate heat from the VCSELs as both the anode and the cathode contacts are on the surface of the chip. The output end of the GUIDECAST™ OIU is attached to a standard MT-ferrule to couple light into a 10-channel multimode fiber ribbon. Various types of MT-ferrule modules are shown in Fig. 23. The optoelectronic packaging philosophy is based on using robotic passive coupling alignment and polymer material molding to achieve high volume, low cost manufacturing.

The leadframe type GUIDECAST™ OIU has worked sufficiently to transmit data at 155 Mb/channel. When a higher data transmission speed is needed, the leadframe capacitance and inductance and the electrical crosstalk between the copper leads become limiting factors. VCSEL Tape Automated Bonding (TAB) packaging is used to address the problem (115), as shown in Fig. 24. The VCSEL array is directly flip-mounted bonded onto the TAB. The polymer GUIDECAST™ OIU without any copper leads is attached to the VCSEL TAB assembly and functions as a waveguide to couple the VCSEL beams into a 10-channel fiber ribbon through a MT-ferrule. This approach has improved the OPTOBUS™ data link speed performance to 400 Mb/channel and is expected to work well for the next generation OPTOBUS™ data link at 800 Mb/channel.

Vertical cavity surface emitting laser array packaging for data links has also been demonstrated with direct fiber coupling (116–119) or through the use of flexible POLYGUIDE™ (120), as shown in Fig. 25. Passive coupling alignment with POLYGUIDE™ approach has recently been demonstrated (121).

Free space parallel optical interconnect has been demonstrated using 2-D VCSEL arrays (122). A 2-D VCSEL array can be flip-chip bonded onto a silicon or a transparent glass submount using Au/Sn bumps. In a board-to-board free space optical interconnect system, microlens arrays and/or holograms are typically used to collimate and distribute the light beams from the VCSEL arrays on one board to the receiver arrays on the other board. To reduce the packaging complexity, microlens arrays can be integrated directly onto the

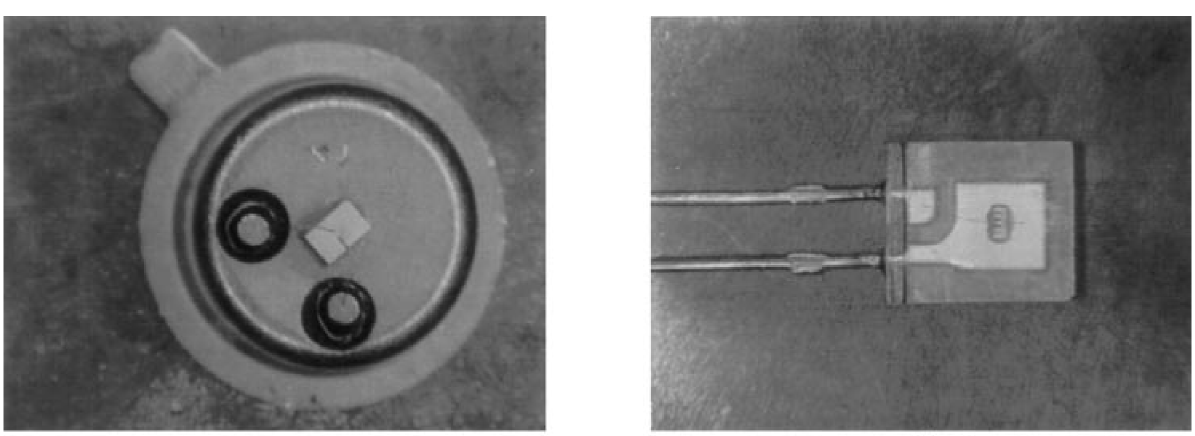

(a) (b)

Figure 21. (a) VCSEL TO can package and (b) VCSEL plastic molded package.

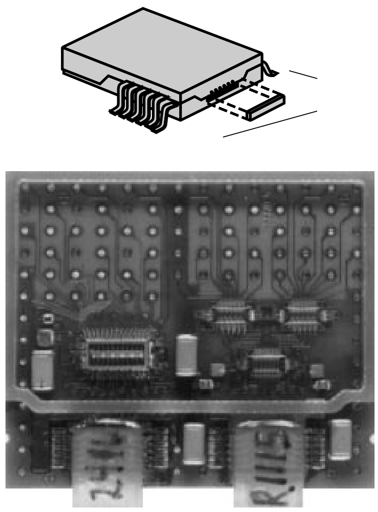

Figure 22. An Optobus® package using a 1 × 10 VCSEL array.

VCSEL arrays. For top emission VCSELs, the integrated microlens may be fabricated using selective oxidation of the AlGaAs method (123) or polyimide reflow technique. For bottom emission VCSELs, such as 980 nm VCSELs or long wavelength VCSELs at 1.3 μm and 1.55 μm, the substrates are transparent. Microlens array can be formed by etching into the transparent substrate (124).

The low cost manufacturing potential and predicated long operation lifetime have also allowed VCSELs to enter the short distance serial optical data link market that has been dominated by the CD lasers and LEDs. LED based optical data links are typically limited to a speed of 100 Mb/s because of the slow carrier recombination lifetime. CD lasers have allowed the optical data link speed to go beyond 100 Mb/s (13,14). However, CD lasers usually have to go through stringent screening to meet the data link reliability requirement. The extra screening procedure increases the laser component cost. In addition, CD lasers usually self-pulsate at around 1 GHz, which prohibits them from being used for high speed data links running above 1 GHz. VCSELs are ideal light sources for gigabit optical data links because of their superb reliability and multigigabit modulation speed capability. Many manufacturers are developing VCSEL based optical data links for a 1.25 Gb/s Ethernet solution. One of the concerns is how to achieve the autopower control (APC) with VCSELs, as 850 nm VCSELs typically used for the data links only emit toward the top surface side because of the absorptive GaAs substrate. The conventional power monitoring scheme for edge emitting semiconductor lasers is not applicable to the VCSELs. One approach is to integrate a p–i–n PD right underneath the VCSEL between the GaAs substrate and the n-DBR (89,100). The p-type doped GaAs substrate is typically used for the device, and the device performance still needs to be improved. In addition, the potential capacitance coupling between the PD and the VCSEL may limit the achievable device speed. The VCSEL APC can also be addressed through the monitoring of scattering VCSEL light in coupling. Figure 26 shows an example in which a large area PD is used to receive the backward scattered light from a ball lens that is used to couple the VCSEL beam into a fiber. The VCSEL power is controlled by monitoring the PD current variation (125). Twin-VCSEL approach has been demonstrated to work well in controlling the primary VCSEL power by monitoring the secondary VCSEL power variation (126). Such a scheme requires that the neighboring VCSELs perform identically to certain degree. The twin-VCSEL APC scheme is extendible to VCSEL arrays, in which one or more VCSELs can be monitored to control the output power of the rest of the VCSELs.

The demand for faster optical data links is pushing for high speed VCSEL packaging technology. Current VCSELs

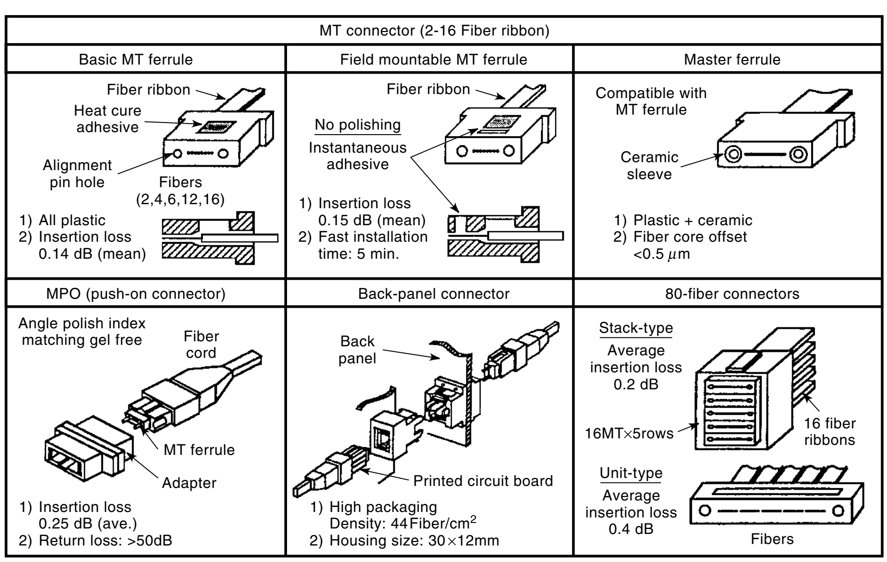

Figure 23. Several types of MT ferrules compatible with VCSEL arrays.

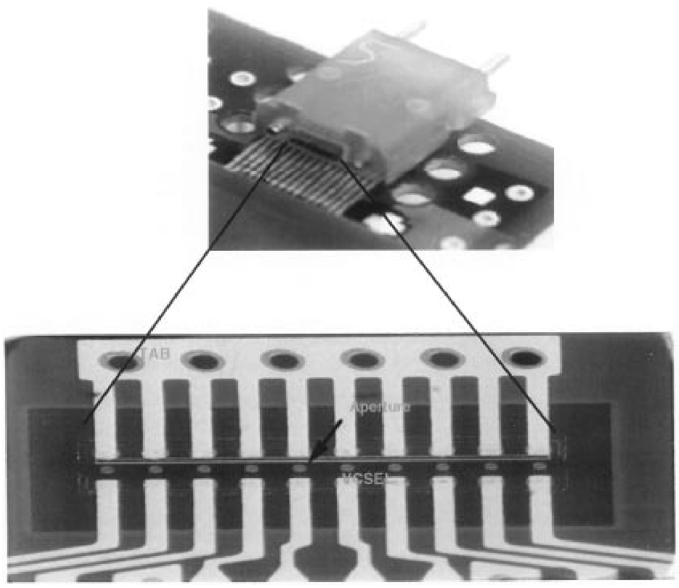

Figure 24. VCSEL packaging using TAB bonding process for Optobus®.

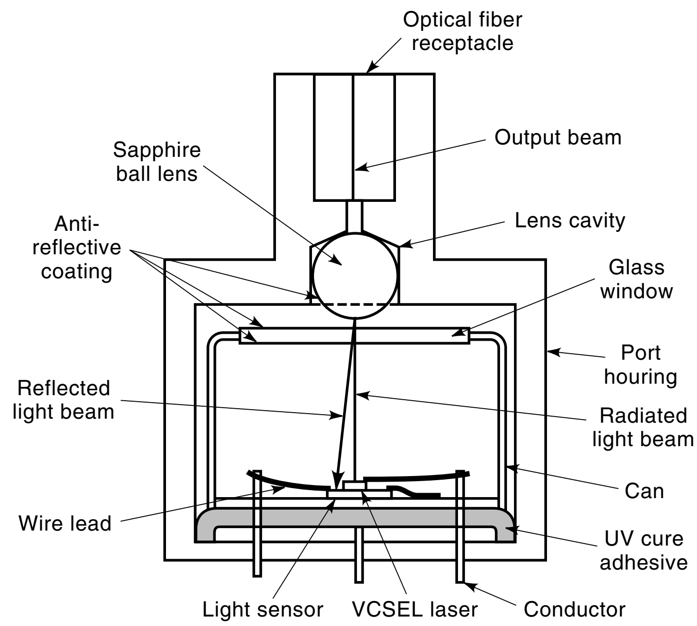

Figure 26. A large area PD is used to receive the backward scattered light for VCSEL auto power control (APC).

used for the serial data links are packaged in TO-metal cans, which put a limit in achievable data link speed due to parasitic capacitance and inductance of the metal packages. Although their series resistance is usually higher than most edge emitting lasers, VCSELs do not generate so much heat because of their low threshold current and low operation current. As a matter of fact, the challenge in VCSEL heat dissipation is mostly on the device design itself as the VCSEL heat is mostly concentrated in a very tiny active region. Typical sizes are conceptually a disk 100 nm thick, 15 μm in diameter, and 2–4 μm beneath the top surface of the chip. One successful attempt in the heat dissipation is to surround the VCSEL active area with a thick layer of gold (127), thus to increase the VCSEL output power. As long as the heat can be effectively dissipated across the whole chip, the heat dissipation requirement for VCSEL packaging is not so demanding. Consequently, plastic molding technology can be adapted to the VCSEL packaging to reduce the packaging related parasitic capacitance and inductance in addition to the cost reduction. For example, a plastic molded VCSEL array packaged on a SO-8 leadframe has been demonstrated with a modulation speed of more than 3 GHz.

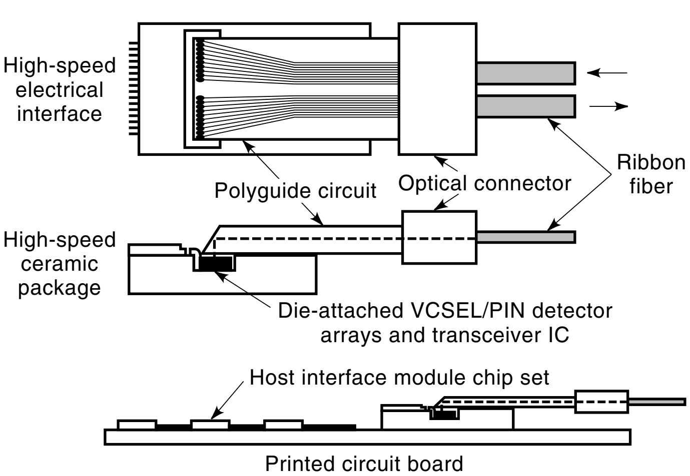

Figure 25. VCSEL array packaging using flexible Polyguide® waveguide.

Recent demonstration of sub-100 μA threshold VCSELs has made photonic very large scale integration possible. Such a technology can be used in achieving Terabit/sec parallel mass data transport optical interconnect. The application presents not only a challenge to the photonic device design but also a challenge to the system packaging, which may somewhat be simplified when electronic integrated circuits (IC) based laser drivers and receiver preamplifiers are integrated with the photonic devices. How successful the photonic very large scale integration can be will rely heavily on how to achieve a high speed low cost system packaging.

PACKAGING PHILOSOPHY AND ROADMAP

Over the last two decades, the evolution in optoelectronic packaging has primarily been focused on supporting fiber optics for telecommunications where the system cost of laying a fiber optic cable many miles across countries and oceans completely outweighed the cost of a transceiver at each end of the fiber. As telecommunications was the first application for semiconductor lasers, the transceiver design and, hence, the package and laser designs were made to be as reliable as technically possible. With the inelastic cost scenario due to the fiber installation, the transceivers had the best materials, the best devices, and a *gold plated* design to form a package platform where reliability was a key design goal for the system. However, over the last two decades, engineers have realized that the semiconductor laser had (and still has) a wide appeal in other applications such as optical storage, bar-code scanners, printers, and so on, where the system design called for lower cost structures of the package platform. The expensive transceiver for telecommunications still has its place in the long distance fiber optic segment, but cannot compete well with consumer applications such as CD-audio, which is extremely cost sensitive. Hence, this led to the development of new package platforms for optoelectronics such as the TO-can which was borrowed and modified from the electronics sector. The TO-can is a de facto standard in cost sensitive semiconductor applications with huge volumes, such as CD players, but has not penetrated the telecommunications market to any extent. Here, the butterfly package is still the dominant package platform for transceivers, although recent trends indicate that innovative solutions such as a silicon wafer board and TAB are being driven to support a new and exciting sector in fiber optic communications: data communications. The data communications arena essentially demands shorter fiber optic links, which in turn place tighter cost pressures on the package platform. Today, there is a mix of butterfly packages for the longwavelength lasers and TO-can for shorter wavelength emitters, but this is not enough: consumers want transceiver costs to fall in line with existing copper solutions! This may or may not be achievable, but the drive and the need is real; engineers have to create optoelectronic package designs in order to generate a sustainable business. With new technologies such as VCSELs, which allow innovative solutions to package platforms, the general trend is the same as the butterfly and the TO-can: plastic packages need not be hermatic; they may include integrated functions (ICs, lenses, leadframes, devices—active and passive, connectors, waveguides), to name the obvious. Plastic packaging has been proven to have lower system costs as is evident by the electronics industry with the common plastic dip (p-dip) in both the surface mount and through-hole configurations. Clearly, with extremely tight cost pressures, as in the indicator businesses as experienced by LEDs, the initial package platform of the TO-can (also borrowed from the silicon industry) has developed into simple dome leadframe plastic packaging where simplicity is key. LEDs have largely been successful in sustaining a good business using plastic molding as a package platform for 100 of millions of units where fractions of a cent may have a dramatic effect on a business strategy. The applications for LEDs have never really required high speed designs, although commercial LED products do exist in the 500 Mbps range, expensive IC drivers and more complicated packages need to be used (such as the TO-can and butterfly). Clearly, plastic based package platforms are the future direction for all optoelectronics devices as evidenced by the LED industry. There is now an expectation of significant plastic penetration into semiconductor based applications and more borrowing from the electronics industry with technologies such as TAB, flip-chip, leadless carriers, etc., that will become more common-place in the coming years.

The roadmap for optoelectronics packaging is still evolving as market forces drive the cost structures and the designs, but clear directions in major applications can be identified. In the high speed, high reliability telecommunications industry, automation of assembly is a major thrust; for example, traditional hand-aligned single-mode lasers are labor intensive due to submicron alignment tolerances between fiber and laser. Here, the butterfly platform is expected to survive but perhaps with a different form factor. Gradually, the hand-built actively aligned (i.e., with the laser turned on) packages of today will be assembled automatically using passive alignment (i.e., laser turned off), and then standard design features (e.g., hematicity, thermal, mechanical, and connector, etc.) will be innovated to include more plastic and more silicon with less process steps and simpler manufacturing. Pig-tailing is common-place today using active alignment but will evolve to connectorized packages and assembled with tighter tolerances and higher quality using passive alignment and robotics. In data communications where local area networks, interconnect links between premises, within premises, etc. become more prevalent, the package design of butterfly and TO today will evolve to plastic dip, pin grid array, and ball grid array platforms where size, performance, and cost will be the key drivers. These designs will drive the higher performance packages used in the telecommunications industry to look at lower cost solutions. Pig-tailing is expected to be suppressed by connectorized packages that have built-in connectors and lenses using a combination of injected and transfer molding techniques. Diffractive and refractive designs in the optics is expected to reduce the reliance on glass lenses today. Another direction in the telecommunications industry is the development of the expanded beam edge emitting laser, which essentially matches the input single mode fiber core numerical aperture for more efficient optical coupling. This will allow lower cost automated passive alignment pig-tail packaging. In the optical storage industry presently, there is a trend to integrated plastic packages which house devices, lenses, and chip carriers with a new form of I/O (input/output) interface. Designers have realized that packages borrowed from the electronics industry such as the TO-can, when manufactured in high volumes, such as CD applications, have a cost that can be scaled in optoelectronics similar to early transistor TO-cans. This means that to add value to the package, more functions need to be integrated, that is, climb the value chain. This is a very clear direction in all optoelectronic package platforms: adding value through integration. Obviously, the designer must be aware of the electronics industries traditional bottlenecks such as increasing I/O with pin-outs, but with the opportunity of using optics as a I/O interface, different and innovative solutions will emerge to provide higher density, lower cost, and integrated plastic packages. In LED type industries, this trend is common-place for visible arrays of LEDs in dot matrix package platforms used for alpha-numerics, etc. The value of packaging a plurality of LEDs has given system designers an opportunity to increase value in the package and generate more profit. The direction is again toward an integrated plastic package where in LED applications, the major missing components might well be silicon IC drivers, multiplexors for reduced I/O, etc., that automatically increase the value of the package.

Lastly, a new philosophy in integrated plastic package design is emerging: trying to design optoelectronic package solutions that will fit onto existing electronic industries assembly lines, without the need to commission custom tooling for optoelectronics. Today, the optoelectronics industry uses essentially custom assembly tooling designed to handle the tight tolerancing required of all opto components, especially single mode lasers for telecommunications where typical tolerancing is a few microns of a meter. This can be balanced with the traditional tolerancing experiences by a p-dip in electronics, where 75 microns is typical. Custom tooling is prohibitively expensive compared to production tools for p-dips as manufacturing factories are commonplace. The challenge today is to use design engineering innovation to effectively utilize existing electronics assembly tooling for more demanding optoelectronics assembly by addressing new package platforms: Integrated plastic packaging is clearly on the roadmap for future optoelectronic packages be they laser, VCSEL, or LED.

BIBLIOGRAPHY

1. J. Gowar, *Optical Communication Systems,* Englewood Cliffs, NJ: Prentice Hall, 1984.
2. S. E. Miller and A. G. Chynoweth (eds.), *Optical Fiber Telecommunications,* New York: Academic Press, 1979.
3. R. Lasky, U. Osterberg, and D. Stigliani (eds.), *Optoelectronics for Data Communication,* New York: Academic Press, 1995.
4. R. R. Tummala, E. J. Rymaszewski, and A. G. Klopfenstein, *Microelectronics Packaging Handbook,* 2nd ed., New York: Chapman & Hall, 1989.
5. R. N. Hall et al., Coherent light emission from GaAs junctions, *Phys. Rev. Lett.,* **9**: 336, 1962.
6. M. I. Nathan et al., Stimulated emission of radiation from GaAs p-n junctions, *Appl. Phys. Lett.,* **1**: 62, 1962.
7. N. Holonyak, Jr. and S. F. Bevacqua, Coherent (visible) light emission from $Ga(Al_{1-x}P_x)As$ junctions, *Appl. Phys. Lett.,* **1**: 82, 1962.
8. T. M. Quist et al., Semiconductor maser of GaAs, *Appl. Phys. Lett.,* **1**: 91, 1962.
9. H. Kroemer, A proposed class of heterojunction injection lasers, *Proc. IEEE,* **51**: 1782, 1963.
10. I. Hayashi et al., Junction lasers which operate continuously at room temperature, *Appl. Phys. Lett.,* **17**: 109, 1970.
11. Zh. I. Alferov et al., Investigation of the influence of the AlAs-GaAs heterostructure parameters on the laser threshold current and the realization of continuous emission at room temperature, *Sov. Phys. Semicond.,* **4**: 1573, 1971.
12. S. G. Anderson, Annual review of laser markets, *Laser Focus World,* **32**: 50, 1996.
13. W. H. Cheng and J. H. Bechtel, High-speed fibre optic links using 780 nm compact disc lasers, *Electron. Lett.,* **29**: 2055, 1993.
14. R. L. Soderstrom et al., CD lasers optical data links for workstations and midrange computers, *ECTC '93,* 505, Orlando, FL, June, 1993.
15. N. Nakata, Laser diodes have low noise and low astigmatism, *JEE,* 49. Aug., 1987.
16. S. Wang, *Fundamentals of Semiconductor Theory and Device Physics,* Englewood Cliffs, NJ: Prentice Hall, 1989.
17. P. A. Morton et al., 25 GHz bandwidth 1.55-μm GaInAsP p-doped strained multiquantum-well lasers, *Electron. Lett.,* **29**: 136, 1993.
18. J. D. Ralston et al., Advanced epitaxial growth and device processing techniques for ultrahigh-speed (>40 GHz) directly modulated semiconductor lasers, *Proc. SPIE,* **2683**: 30, 1996.
19. J. J. Coleman, Quantum-well heterostructure lasers. In G. P. Agrawal (ed.), *Semiconductor lasers: past, present, and future,* Ch. 1. Woodbury, NY: AIP Press, 1995.
20. R. Nagarajan et al., High-speed InGaAs/GaAs strained multiple quantum well lasers with low damping, *Appl. Phys. Lett.,* **58**: 2326, 1991.
21. B. I. Miller et al., Strain-compensated strained-layer superlattices for 1.5 μm wavelength lasers, *Appl. Phys. Lett.,* **58**: 1952, 1991.
22. G. Zhang and A. Ovtchinnikov, Strain-compensated InGaAs/GaAsP/GaInAsP/GaInP quantum well lasers ($1 \sim 0.98$ μm) grown by gas-source molecular beam epitaxy, *Appl. Phys. Lett.,* **62**: 1644, 1993.
23. T. Tsuchiya et al., Investigation of effect of strain-compensated structure and compensation limit in strained-layer multiple quantum wells, *J. Cryst. Growth,* **145**: 371, 1994.
24. Y. Bessho et al., Self-pulsating 630 nm band strain-compensated MQW AlGaInP laser diodes, *Electron. Lett.,* **32**: 667, 1996.
25. S. R. Nagel, J. B. MacChesney, and K. L. Walker, Modified chemical vapor deposition, in T. Y. Li (ed.), *Optical Fiber Communications,* **1**, Orlando: Academic Press, 1985.
26. L. G. Cohen, C. Lin, and W. G. French, Tailoring zero chromatic dispersion into the 1.5–1.6 μm low-loss spectral region of single-mode fibres, *Electron. Lett.,* **15**: 334, 1979.
27. H. Tsuchiya and N. Imoto, Dispersion-free single-mode fibre in 1.5 μm wavelength region, *Electron. Lett.,* **15**: 476, 1979.
28. K. Okamoto et al., Dispersion minimisation in single-mode fibres over a wide spectral range, *Electron. Lett.,* **15**: 729, 1979.
29. J. J. Hsieh, J. A. Rossi, and J. P. Donnelly, Room-temperature cw operation of GaInAsP/InP double-heterostructure diode lasers emitting at 1.1 μm, *Appl. Phys. Lett.,* **28**: 709, 1976.
30. R. J. Nelson et al., High-output power InGaAsP ($1 = 1.3$ μm) strip-buried heterostructure lasers, *Appl. Phys. Lett.,* **36**: 358, 1980.
31. M. Hirao et al., Long wavelength InGaAsP/InP lasers for optical fiber communication systems, *J. Opt. Commun.,* **1**: 10, 1980.
32. N. K. Dutta and R. J. Nelson, The case for Auger recombination in $In_{1-x}Ga_xAs_yP_{1-y}$, *J. Appl. Phys.,* **53**: 74, 1982.
33. N. K. Dutta et al., Long wavelength InGaAsP ($1 \sim 1.3$ μm) modified multiquantum well laser, *Appl. Phys. Lett.,* **46**: 1036, 1985.
34. R. J. S. Bates and S. D. Walker, Evaluation of all-plastic optical fibre compute data link dispersion limits, *Electron. Lett.,* **28**: 996, 1992.
35. P. Gwynne, Digital video disk technology offers increased storage features, *R&D Magazine,* **38**: 40, Aug., 1996.
36. S. Yamamoto et al., Room-temperature cw operation in the visible spectral range of 680–700 nm by AlGaAs double heterojunction lasers, *Appl. Phys. Lett.,* **41**: 796, 1982.
37. A. Usui et al., Room temperature cw operation of visible InGaAsP double heterostructure laser at 671 nm grown by hydride VPE, *Jpn. J. Appl. Phys.,* **24**: L163, 1985.
38. T. H. Chong and K. Kishino, Room temperature continuous wave operation of 671-nm wavelength GaInAsP/AlGaAs VSIS lasers, *IEEE Photon. Technol. Lett.,* **2**: 91, 1990.
39. K. Kobayashi et al., Room-temperature cw operation of AlGaInP double-heterostructure visible lasers, *Electron. Lett.,* **21**: 931, 1985.
40. M. Ikeda et al., Room-temperature continuous-wave operation of an AlGaInP double heterostructure laser grown by atmospheric pressure metalorganic chemical vapor deposition, *Appl. Phys. Lett.,* **47**: 107, 1985.
41. M. Ishikawa et al., Room-temperature cw operation of InGaP/InGaAlP visible light laser diodes on GaAs substrates grown by metalorganic chemical vapor deposition, *Appl. Phys. Lett.,* **48**: 207, 1986.
42. G. Hatakoshi et al., High-temperature operation of high-power InGaAlP visible laser, *Proc. SPIE,* **1850**: 388, 1993.
43. J. Hashimoto et al., Effects of strained-layer structures on the threshold current density of AlGaInP/GaInP visible lasers, *Appl. Phys. Lett.,* **58**: 879, 1991.
44. S. Honda et al., Transverse-mode stabilized 630 nm-band AlGaInP strained multiquantum-well laser diodes grown on misoriented substrates, *Electron. Lett.,* **28**: 1365, 1992.

45. T. Tanaka et al., High-temperature operation of 637 nm AlGaInP MQW laser diodes with quaternary QWS grown on misoriented substrates, *Electron. Lett.,* **29**: 24, 1993.

46. Y. Ueno et al., 30-mW 690-nm high-power strained-quantum-well AlGaInP laser, *IEEE J. Quantum Electron.,* **QE-29**: 1851, 1993.

47. S. Arimoto et al., 150 mW fundamental-transverse-mode operation of 670 nm window laser diode, *IEEE J. Quantum Electron.,* **QE-29**: 1874, 1993.

48. N. Nakayama et al., Room temperature continuous operation of blue-green laser diodes, *Electron. Lett.,* **29**: 1488, 1993.

49. J. M. Gaines et al., Blue-green injection lasers containing pseudomorphic $Zn_{1-x}Mg_xS_ySe_{1-y}$ cladding lasers and operating up to 394 K, *Appl. Phys. Lett.,* **62**: 2462, 1993.

50. M. A. Haase et al., Wu, Low-threshold buried-ridge II-VI laser diodes, *Appl. Phys. Lett.,* **63**: 2315, 1993.

51. S. Taniguchi et al., 100 h II-VI blue-green laser diode, *Electron. Lett.,* **32**: 552, 1996.

52. S. Nakamura, T. Mukai, and M. Senoh, High-power GaN p-n junction blue-light-emitting diodes, *Jpn. J. Appl. Phys.,* **30**: L1998, 1991.

53. S. Nakamura et al., InGaN MQW structure laser diodes with cleaved mirror facets, *Jpn J. Appl. Phys.,* **35**: L217, 1996.

54. K. Itaya et al., Room temperature pulsed operation of nitride based multi-quantum-well laser diodes with cleaved facets on conventional c-face sapphire substrates, *Jpn. J. Appl. Phys.,* Part 2, **35**: L1315, 1996.

55. I. Akasaki et al., Shortest wavelength semiconductor laser diode, *Electron. Lett.,* **32**: 1105, 1996.

56. S. Nakamura et al., InGaN multi-quantum-well structure laser diodes grown on $MgAl_2O_4$ substrates, *Appl. Phys. Lett.,* **68**: 2105, 1996.

57. I. Akasaki and H. Amano, Progress and future prospects of group III nitride semiconductors, *LEOS '96,* Plen 2, Boston, MA, Nov., 1996.

58. S. Nakamura et al., First room-temperature continuous-wave operation of InGaN multi-quantum-well-structure laser diodes, *LEOS '96,* PD1.1, Boston, MA, Nov., 1996.

59. H. Soda et al., GaInAsP/InP surface emitting injection lasers, *Jpn. J. Appl. Phys.,* **18**: 2329, 1979.

60. K. Iga, F. Koyama, and S. Kinoshita, Surface emitting semiconductor lasers, *IEEE J. Quantum Electron.,* **QE-24**: 1845, 1988.

61. M. Lebby et al., Use of VCSEL arrays for parallel optical interconnects, *Proc. SPIE,* **2683**: 81, 1996.

62. M. Orenstein et al., Matrix addressable vertical cavity surface emitting laser array, *Electron. Lett.,* **27**: 437, 1991.

63. C. L. Shieh, D. E. Ackley, and H. C. Lee, Temperature insensitive vertical cavity surface emitting laser, U.S. Patent #5,274,655, 1993.

64. D. B. Young et al., High-power temperature-insensitive gain-offset InGaAs/GaAs vertical-cavity surface-emitting lasers, *IEEE Photon. Technol. Lett.,* **5**: 129, 1993.

65. K. Tai et al., 90% coupling of top surface emitting GaAs/AlGaAs quantum well laser output into 8 μm diameter core silica fibre, *Electron. Lett.,* **26**: 1628, 1990.

66. K. Iga et al., Room temperature pulsed oscillation of GaAlAs/GaAs surface emitting laser, *Appl. Phys. Lett.,* **45**: 348, 1984.

67. F. Koyama, S. Kinoshita, and K. Iga, Room-temperature CW operation of GaAs vertical cavity surface emitting laser, *Trans. IEICE,* **E71**: 1089, 1988.

68. F. H. Peters et al., High power vertical cavity surface emitting lasers, *Electron. Lett.,* **29**: 200, 1993.

69. M. Grabherr et al., High power top-surface emitting oxide confined vertical-cavity laser diodes, *Electron. Lett.,* **32**: 1723, 1996.

70. D. L. Huffaker, J. Shin, and D. G. Deppe, Low threshold half-wave vertical-cavity lasers, *Electron. Lett.,* **30**: 1946, 1994.

71. G. M. Yang, M. H. MacDougal, and P. D. Dapkus, Ultralow threshold current vertical-cavity surface-emitting lasers obtained with selective oxidation, *Electron. Lett.,* **31**: 886, 1995.

72. K. L. Lear et al., Selectively oxidised vertical cavity surface emitting lasers with 50% power conversion efficiency, *Electron. Lett.,* **31**: 208, 1995.

73. B. Weigl et al., High performance oxide-confined GaAs VCSEL's, *IEEE J. Selected Top. Quantum Electron.,* **3**: 409, 1997.

74. K. Iga, Surface emitting lasers, *Opt. Quantum Electron.,* **24**: S97, 1992.

75. D. I. Babic et al., Room-temperature continuous-wave operation of 1.54-μm vertical-cavity lasers, *IEEE Photon. Technol. Lett.,* **7**: 1225, 1995.

76. N. M. Margalit et al., Submilliamp long wavelength vertical cavity lasers, *Electron. Lett.,* **32**: 1675, 1996.

77. D. Vakhshoori et al., 8 $\times$ 18 top emitting independently addressable surface emitting laser arrays with uniform threshold current and low threshold voltage, *Appl. Phys. Lett.,* **62**: 1718, 1993.

78. S. Uchiyama and K. Iga, Two-dimensional array of GaInAsP/InP surface-emitting lasers, *Electron. Lett.,* **21**: 162, 1985.

79. D. G. Deppe et al., Phase-coupled two-dimensional $Al_xGa_{1-x}As$-GaAs vertical-cavity surface-emitting laser array, *Appl. Phys. Lett.,* **56**: 2089, 1990.

80. M. Orenstein et al., Two-dimensional phase-locked arrays of vertical-cavity semiconductor lasers by mirror reflectivity modulation, *Appl. Phys. Lett.,* **58**: 804, 1991.

81. G. Hasnain et al., Continuous wave top surface emitting quantum well lasers using hybrid metal/semiconductor reflectors, *Electron. Lett.,* **26**: 1590, 1990.

82. R. A. Morgan et al., 200 degrees-C, 96-nm wavelength range, continuous-wave lasing from unbonded GaAs MOVPE-grown vertical cavity surface-emitting lasers, *IEEE Photon. Technol. Lett.,* **7**: 441, 1995.

83. P. Zhou et al., Low series resistance high-efficiency GaAs/AlGaAs vertical-cavity surface-emitting lasers with continuously graded mirrors grown by MOCVD, *IEEE Photon. Technol. Lett.,* **3**: 591, 1991.

84. J. J. Dudley, D. L. Crawford, and J. E. Bowers, Temperature dependence of the properties of DBR mirrors used in surface normal optoelectronic devices, *IEEE Photon. Technol. Lett.,* **4**: 311, 1992.

85. M. Lebby et al., Vertical-cavity surface-emitting lasers for communication applications, *OSA Annual '96,* WR1, Rochester, NY, October, 1996.

86. M. R. T. Tan et al., Surface emitting laser for multimode data link applications, *HP J.,* **67**, Feb., 1995.

87. Y. H. Lee et al., Deep-red CW top surface-emitting vertical-cavity AlGaAs superlattice lasers, *IEEE Photon. Technol. Lett.,* **3**: 108, 1991.

88. H. E. Shin et al., 780 nm oxidised vertical-cavity surface-emitting lasers with $Al_{0.1}Ga_{0.89}As$ quantum wells, *Electron. Lett.,* **32**: 1287, 1996.

89. T. Kim et al., A single transverse mode operation of top surface emitting laser diode with an integrated photo-diode, *Proc. LEOS '95,* **2**: 416, San Francisco, CA, 1995.

90. R. P. Schneider, Jr. et al., Efficient room-temperature continuous-wave AlGaInP/AlGaAs visible (670 nm) vertical-cavity surface-emitting laser diodes, *IEEE Photon. Technol. Lett.,* **6**: 313, 1994.

91. K. D. Choquette et al., Continuous wave operation of 640–660 nm selectively oxidised AlGaInP vertical-cavity lasers, *Electron. Lett.,* **31**: 1145, 1995.

92. R. P. Schneider, Jr. et al., Improved AlGaInP-based red (670–690 nm) surface-emitting lasers with novel C-doped short-cavity epitaxial design, *Appl. Phys. Lett.,* **67**: 329, 1995.

93. M. H. Crawford et al., Temperature-dependent characteristics and single-mode performance of AlGaInP-based 670–690-nm vertical-cavity surface-emitting lasers, *IEEE Photon. Technol. Lett.,* **7**: 724, 1995.

94. T. Baba et al., Near room temperature continuous wave lasing characteristics of GaInAsP/InP surface emitting laser, *Electron. Lett.,* **29**: 913, 1993.

95. J. J. Dudley et al., 144 °C operation of 1.3 μm InGaAsP vertical cavity lasers on GaAs substrates, *Appl. Phys. Lett.,* **61**: 3905, 1992.

96. J. J. Dudley et al., Low threshold, wafer fused long wavelength vertical cavity lasers, *Appl. Phys. Lett.,* **64**: 1463, 1994.

97. H. K. Shin et al., Vertical-cavity surface-emitting lasers for optical data storage, *Jpn. J. Appl. Phys.,* Part 1, **35**: 506, 1996.

98. G. Hasnain and K. Tai, Self-monitoring semiconductor laser device, U.S. Patent #5,136,603, 1992.

99. G. Hasnain et al., Monolithic integration of photodetector with vertical cavity surface emitting laser, *Electron. Lett.,* **27**: 1630, 1991.

100. M. K. Hibbs-Brenner, Integrated laser power monitor, U.S. Patent #5,475,701, 1995.

101. G. Bjork and Y. Yamamoto, Analysis of semiconductor microcavity lasers using rate equations, *IEEE J. Quantum Electron.,* **QE-27**: 2386, 1991.

102. R. J. Ram et al., Spontaneous emission factor in post microcavity lasers, *IEEE Photon. Technol. Lett.,* **8**: 599, 1996.

103. D. L. Huffaker, D. G. Deppe, and K. Kumar, Native-oxide ring contact for low threshold vertical-cavity lasers, *Appl. Phys. Lett.,* **65**: 97, 1994.

104. M. H. MacDougal et al., Ultralow threshold current vertical-cavity surface-emitting lasers with AlAs oxide-GaAs distributed Bragg reflectors, *IEEE Photon. Technol. Lett.,* **7**: 229, 1995.

105. M. H. MacDougal et al., Electrically-pumped vertical-cavity lasers with Al_xO_y-GaAs reflectors, *IEEE Photon. Technol. Lett.,* **8**: 310, 1996.

106. K. L. Lear et al., High frequency modulation of oxide-confined vertical cavity surface emitting lasers, *Electron. Lett.,* **32**: 457, 1996.

107. B. J. Thibeault et al., High-speed characteristics of low-optical loss oxide-apertured vertical-cavity lasers, *IEEE Photon. Technol. Lett.,* **9**: 11, 1997.

108. R. Bonda et al., Physical design and assembly process development of a multi-chip package containing a light emitting diode (LED) array die, *Proc. 46th Electron. Comp. Technol. Conf.,* 1039, 1996.

109. A. P. R. Harpin, Solving packaging issues for low-cost Si integrated optical components, *Proc. LEOS '96,* **2**: 102, 1996.

110. G. K. Khoe and G. Kuyt, Realistic efficiency of coupling light from GaAs laser diode into parabolic-index optical fibers, *Electron. Lett.,* **14**: 667, 1978.

111. L. A. Reith, P. W. Shumate, and Y. Koga, Laser coupling to single-mode fibre using graded-index lenses and compact disk 1.3 μm laser package, *Electron. Lett.,* **22**: 836, 1986.

112. K. Mathyssek, J. Wittmann, and R. Keil, Fabrication and investigation of drawn fiber tapers with spherical microlenses, *J. Opt. Commun.,* **6**: 142, 1985.

113. C. A. Armiento et al., Passive coupling of InGaAsP/InP laser array and singlemode fibres using silicon waferboard, *Electron. Lett.,* **27**: 1109, 1991.

114. Q. Tan and Y. C. Lee, Soldering technology for optoelectronic packaging, *Proc. 46th Electron. Compon. Technol. Conf.,* 26, 1996.

115. M. L. Lebby et al., Key challenges and results of VCSELs in data links, *LEOS '96,* WV2, Boston, MA, Nov., 1996.

116. E. Zeeb et al., Planar proton implanted VCSEL's and fiber-coupled 2-D VCSEL arrays, *IEEE J. Sel. Top. Quantum Electron.,* **1**: 616, 1995.

117. Y. M. Wong et al., Technology development of a high-density 32-channel 16-Gb/s optical data link for optical interconnection applications for the optoelectronic technology consortium (OETC), *J. Lightwave Technol.,* **13**: 995, 1995.

118. H. Kosaka et al., Gigabit-rate optical-signal transmission using vertical-cavity surface-emitting lasers with large-core plastic-cladding fibers, *IEEE Photon. Technol. Lett.,* **7**: 926, 1995.

119. K. Matsuda et al., A surface-emitting laser array with backside guiding holes for passive alignment to parallel optical fibers, *IEEE Photon. Technol. Lett.,* **8**: 494, 1996.

120. K. H. Hahn, POLO—Parallel optical links for gigabyte data communication, *Proc. 45th ECTC,* 368, Las Vegas, NV, May, 1995.

121. J. R. Rowlette, Jr. et al., Laser micromachining of polymer waveguides for low cost passive alignment to VCSELs, *Proc. LEOS '96,* **2**: 169, 1996.

122. R. F. Carson et al., Low-power, parallel photonic interconnections for multi-chip module applications, *Proc. 45th ECTC,* 380, 1995.

123. O. Blum et al., Buried refractive microlenses formed by selective oxidation of AlGaAs, *Electron. Lett.,* **32**: 1406, 1996.

124. E. M. Strzelecka et al., Monolithic integration of vertical-cavity laser diodes with refractive GaAs microlenses, *Electron. Lett.,* **31**: 724, 1995.

125. M. A. Gottschalk, Optical data link delivers more for less, *Design News,* **120**, March, 1997.

126. W. B. Jiang et al., Vertical cavity surface emitting laser packaging with auto power control, *Proc. 47th ECTC,* 368, 1997.

127. T. Wipiejewski et al., High performance vertical-cavity surface-emitting laser diodes with a Au-plated heat spreading layer, *Proc. 45th ECTC,* 401, 1995.

WENBIN JIANG
MICHAEL S. LEBBY
Motorola, Inc.